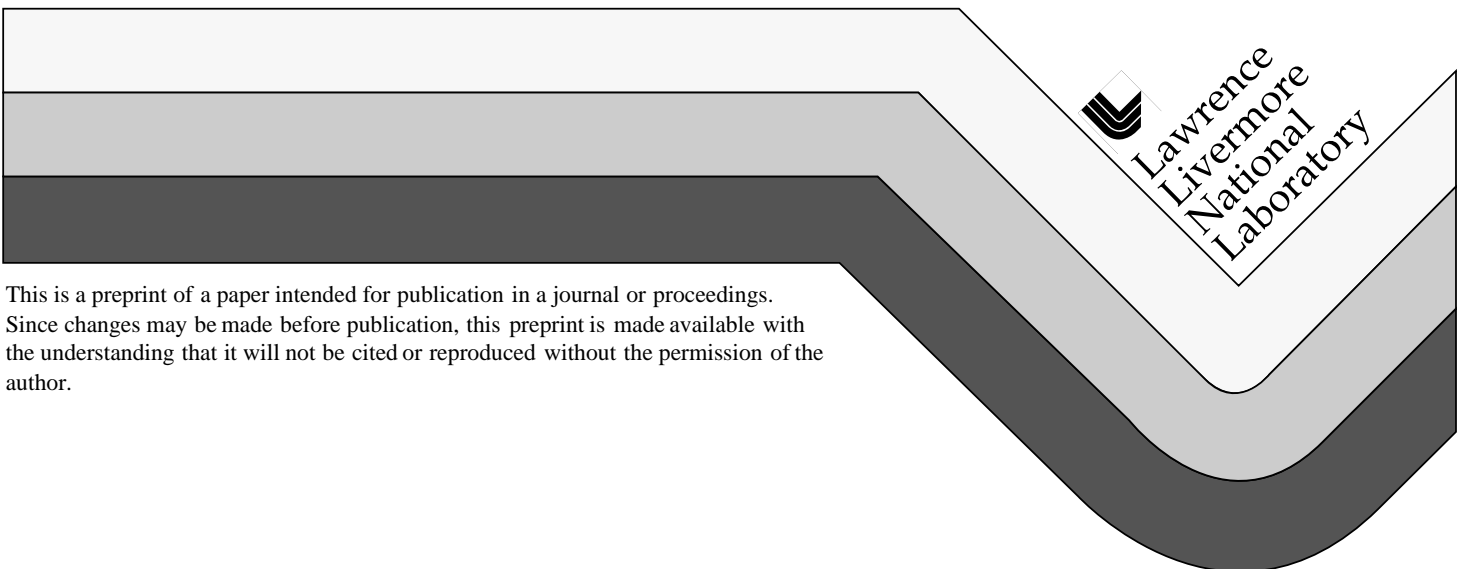


# A New Laser Driver for Physics Modeling Codes using Unstructured 3D Grids

T. B. Kaiser, J. L. Milovich, A. I. Shestakov, M. K. Prasad

This paper was prepared for submittal to the  
1998 Nuclear Explosives Development Conference  
Las Vegas, NV  
October 25-30, 1998

February 2, 1999



This is a preprint of a paper intended for publication in a journal or proceedings.  
Since changes may be made before publication, this preprint is made available with  
the understanding that it will not be cited or reproduced without the permission of the  
author.

#### DISCLAIMER

This document was prepared as an account of work sponsored by an agency of the United States Government. Neither the United States Government nor the University of California nor any of their employees, makes any warranty, express or implied, or assumes any legal liability or responsibility for the accuracy, completeness, or usefulness of any information, apparatus, product, or process disclosed, or represents that its use would not infringe privately owned rights. Reference herein to any specific commercial product, process, or service by trade name, trademark, manufacturer, or otherwise, does not necessarily constitute or imply its endorsement, recommendation, or favoring by the United States Government or the University of California. The views and opinions of authors expressed herein do not necessarily state or reflect those of the United States Government or the University of California, and shall not be used for advertising or product endorsement purposes.

# A New Laser Driver for Physics Modeling Codes using Unstructured 3D Grids

T. B. Kaiser, J. L. Milovich, A. I. Shestakov and M. K. Prasad  
*Lawrence Livermore National Laboratory,  
University of California,  
Livermore, CA 94550*

February 2, 1999

## Abstract

We present a status report on the current state of development, testing and application of a new scheme for laser beam evolution and power deposition on three-dimensional unstructured grids. The scheme is being encapsulated in a C++ library for convenient porting to existing modeling codes. We have added a new ray propagator that is second order in time, allowing rays to refract within computational zones as well as at zone interfaces. In a globally constant free-electron density gradient on a randomized hexahedral mesh, the new integrator produces ray trajectories that agree with analytic results to within machine roundoff. A new method for computing the inverse-bremsstrahlung energy deposition rate that captures its highly non-uniform spatial dependence within a zone has also been added. This allows accurate trajectories without the necessity of sub-stepping in time. Other enhancements (not discussed) include multiple user-configurable beams, computation of the electron oscillation velocity in the laser electric field and energy-deposition accounting. Results of laser-driven simulations are presented in a companion paper.

## 1 Introduction

In modeling the propagation and power deposition of laser light in transparent materials one is faced with the usual tradeoff between accuracy and computational efficiency. While solution of the full wave equation preserves all physical effects it is computationally expensive. Geometrical optics, while giving up certain effects (diffraction and polarization, in particular) captures most of the physics of interest (refraction and power deposition and even some ponderomotive effects), is relatively fast, and consequently is the method of choice. Given a ray-tracing approach, unstructured grids pose a problem by complicating the determination of where rays cross computational-zone interfaces, an issue for both ray propagation and power deposition. In some formulations of hydrodynamics, for example discontinuous-finite-elements, the matter density is discontinuous at zone interfaces, which leads to singularities in the effective force governing ray propagation. Proper treatment of these singularities is crucial to accurate modeling of refraction. In an earlier treatment[1] rotational symmetry of the propagating medium was assumed, and two-dimensional quadrilateral zones were triangulated to obtain material properties that varied linearly in the radial and axial coordinates within a zone and were continuous across zone interfaces. Azimuthal ray motion was discretized by assuming constancy of the gradient of the index of refraction during a propagation sub time step, and iterative numerical root-finding used to locate interface crossings.

The present work makes no assumptions about symmetry of the medium. Faces of the three-dimensional zones can be triangular or quadrilateral and have arbitrary orientation. Rays traverse a zone in a single time

step whose length is determined analytically, *i.e.*, iteration is not necessary. Constancy of the effective force governing ray motion within a zone is assumed, but accuracy is controlled by grid resolution rather than by restricting the time step. No requirement of continuity of material properties at zone interfaces is imposed.

An outline of the remainder of the paper is as follows. Section 2 gives a brief summary of the relevant results of geometrical optics, from which is derived the equation of motion of a ray. It is shown that ray propagation is completely determined by the electron density gradient. If the ratio of the zone size to the gradient scale length is adopted as a small parameter, variation of the electron density within a computational zone can be represented as

$$n_e(\vec{x}) = \langle n_e \rangle + \langle \nabla n_e \rangle \cdot (\vec{x} - \langle \vec{x} \rangle) + O(\epsilon^2) \quad (1)$$

where  $\langle \cdot \rangle$  denotes a zone average. In this approximation the density gradient is constant within the zone, so the ray feels a constant force that causes it to move along a parabolic trajectory. In making the transition to the next zone (where the density computed from Eq.(1) is, in general, different) the ray experiences a delta-function effective force normal to the zone interface, which discontinuously changes the component of its velocity normal to the interface, *i.e.*, the transition is governed by Snell's law. In Section 3 the general problem of determining the point of intersection of a ray with a zone face is considered. The equation of an arbitrary quadrilateral zone interface is given. This is used to compute the face unit-normal vector, required for application of Snell's law, and to determine the point of intersection of a ray with a zone interface. Section 4 discusses power deposition by inverse bremsstrahlung. In Section 5 static test cases are given to illustrate the accuracy of the ray tracing and power deposition algorithms. Finally, Section 6 gives a summary of current functionality and implementation status.

## 2 Geometrical Optics

In the geometrical optics approximation[2] electromagnetic wave quantities are written in the form

$$\phi = \hat{\phi}(\vec{x}, t) \exp\{i\omega[S(\vec{x})/c - t]\}, \quad (2)$$

with  $\hat{\phi}$  a slowly-varying amplitude and the exponential phase a large quantity. Retention of the dominant terms when the form (2) is substituted into the wave equation leads to the fundamental equation of geometrical optics,  $|\nabla S|^2 = \eta^2$ , where  $\eta$  is the index of refraction, assumed to vary on a much longer spatial scale than the wavelength of the light. We further assume that  $\eta$  is constant on the ray-transit time scale, *i.e.*, the medium is "frozen" during the time required for a typical ray to traverse the grid. The spatially-dependent part of the phase, or *eikonal*, is related to the local wave vector  $\vec{k}$  by  $\vec{k} = (\omega/c)\nabla S$ . Wavefronts, surfaces of constant phase, move at the phase velocity,  $\omega/|\vec{k}| = c/|\nabla S|$ , while rays, which trace out curves that are everywhere normal to wavefronts, *i.e.*, parallel to  $\nabla S$ , can be thought to progress at the group velocity,  $\vec{v} = c\nabla S$ , the velocity at which energy is transported. The equation of motion of a ray can be obtained by differentiating the group velocity with respect to time[1]:

$$\frac{d^2\vec{x}}{dt^2} = \frac{d\vec{v}}{dt} = c \frac{d\nabla S}{dt} = \nabla \left( \frac{c^2}{2}\eta^2 \right) \quad (3)$$

The index of refraction, or, equivalently for transparent materials, the dielectric function,  $\epsilon = \eta^2$ , is a known function of position for a given material. In a non-relativistic unmagnetized plasma, which for definiteness will be adopted as a model here, it's given by

$$\eta^2 = 1 - \frac{\omega_p^2}{\omega_0^2} = 1 - \frac{n_e}{n_c}, \quad (4)$$

where  $n_c = (m_e/4\pi)(\omega_0/e)^2$  is the critical density, at which the electron plasma frequency  $\omega_p$  equals the laser frequency,  $\omega_0$ . Combining Eq. (4) with Eq. (3) gives the final form of the ray equation of motion:

$$\frac{d^2 \vec{x}}{dt^2} = \nabla \left( -\frac{c^2}{2} \frac{n_e}{n_c} \right). \quad (5)$$

Rays move as unit-mass particles in the potential  $V = (c^2/2) n_e/n_c$ .

### 3 Cell Traversal and Ray Intersection with Zone Interfaces

The equation of a quadrilateral cell interface can be parameterized as follows. Let the positions of the four nodes that define the face be denoted  $\vec{x}_n$ ,  $n = 0, 1, 2, 3$ , the face center  $\langle \vec{x} \rangle \equiv (\vec{x}_0 + \vec{x}_1 + \vec{x}_2 + \vec{x}_3)/4$  and the relative displacements  $\vec{\xi}_m \equiv \vec{x}_m - \vec{x}_0$ ,  $m = 1, 2, 3$ . Then the equation of the face can be shown to be  $\Phi(\vec{x}) = 0$ , where[3]

$$\Phi(\vec{x}) \equiv [(\vec{\xi}_1 \times \vec{\xi}_2 + \vec{\xi}_3 \times \vec{\xi}_1) \cdot (\vec{x} - \langle \vec{x} \rangle)] [(\vec{\xi}_2 \times \vec{\xi}_3 + \vec{\xi}_3 \times \vec{\xi}_1) \cdot (\vec{x} - \langle \vec{x} \rangle)] + [(\vec{\xi}_1 \times \vec{\xi}_2 + \vec{\xi}_2 \times \vec{\xi}_3) \cdot (\vec{x} - \langle \vec{x} \rangle)] \vec{\xi}_1 \cdot (\vec{\xi}_2 \times \vec{\xi}_3)/2 \quad (6)$$

unless  $\vec{\xi}_1 \cdot (\vec{\xi}_2 \times \vec{\xi}_3) = 0$ , in which case the face is planar and  $\Phi$  reduces to the simple form

$$\Phi = (\vec{\xi}_1 \times \vec{\xi}_2 + \vec{\xi}_2 \times \vec{\xi}_3) \cdot (\vec{x} - \langle \vec{x} \rangle). \quad (7)$$

An expression of the same form as (7) holds for triangular faces.

In order to apply Snell's law as a ray crosses a zonal interface the unit vector normal to the interface at the point of intersection is required. Given the equation of the surface, the unit normal is given by  $\hat{u} = \nabla \Phi / |\nabla \Phi|$ , which is simply evaluated from Eq.(6) or(7). The correct sign of  $\hat{u}$  is obtained by requiring that  $\hat{u} \cdot (\vec{x} - \vec{x}_c) > 0$ , where  $\vec{x}_c$  locates the cell center.

Given a ray's position and velocity as it enters a zone, it's exit location and velocity can be determined by substituting its trajectory in the equation of each face bounding the zone and solving for the time at which the trajectory intersects the face. Thus, integration of Eq. (5) gives

$$\vec{v}(\Delta t) = \vec{v}_0 - \frac{c^2}{2n_c} \langle \nabla n_e \rangle \Delta t, \quad (8)$$

$$\vec{x}(\Delta t) = \vec{x}_0 + \vec{v}_0 \Delta t - \frac{c^2}{4n_c} \langle \nabla n_e \rangle (\Delta t)^2, \quad (9)$$

where  $\vec{x}_0$ ,  $\vec{v}_0$  are the entry position and velocity. Substitution of (9) in Eq. (6) for non-planar faces or Eq. (7) for plane faces yields a quartic or quadratic equation, respectively, to be solved for  $\Delta t$ . The smallest positive root obtained in this way is the unique exit time, which when substituted back into Eqs.(8), (9), gives the exit velocity and position. Application of Snell's law then completes determination of the initial conditions for the ray trajectory in the next zone.

### 4 Power Deposition

Because rays are simply curves in space they carry no information about radiation intensity or spatial extent transverse to their direction. Their state is completely defined by their frequency, velocity and power, the latter two attributes of which are, in general, spatially dependent. The power of an electromagnetic wave is depleted as the oscillatory energy it imparts to electrons is randomized by collisions, the inverse-bremsstrahlung process. The rate of energy loss is given by the well-known formula[4]

$$\nu_{ib} = \frac{4}{3} \left( \frac{2\pi}{m_e} \right)^{1/2} \frac{n_e^2 Z e^4 \ln \Lambda}{n_c T_e^{3/2}} \quad (10)$$

where all quantities have their usual meanings and consistent units. As a ray traverses a cell its power decreases with time:

$$P(\Delta t) = P(0) \exp\left\{-\int_0^{\Delta t} dt \nu_{ib}[\vec{x}(t)]\right\} \quad (11)$$

with  $\vec{x}(t)$  given by Eq. (9). Because  $\nu_{ib}$  is such a strongly non-uniform function of position within a cell, care must be taken in computing the integral in Eq.(11). With Eq.(1) for  $n_e[\vec{x}(t)]$  and a similar linear approximation for  $T_e$ , the integrand can be expanded in powers of  $t$ . The result is

$$\int_0^{\Delta t} dt \nu_{ib}[\vec{x}(t)] = C \ln \Lambda \Delta t \left[ 1 + \frac{\langle \nabla n_e \rangle \cdot \vec{v}_0}{\langle n_e \rangle + \langle \nabla n_e \rangle \cdot (\vec{x}_0 - \langle \vec{x} \rangle)} \Delta t - \frac{3}{4} \frac{\langle \nabla T_e \rangle \cdot \vec{v}_0}{\langle T_e \rangle + \langle \nabla T_e \rangle \cdot (\vec{x}_0 - \langle \vec{x} \rangle)} \Delta t \right] + O(\Delta t^3), \quad (12)$$

where

$$C \equiv \frac{4}{3} \left( \frac{2\pi}{m_e} \right)^{1/2} \frac{Z e^4 \langle n_e \rangle^2}{n_c \langle T_e \rangle^{3/2}}. \quad (13)$$

The weak dependence of  $\ln \Lambda$  on  $n_e$ ,  $T_e$  can be included, if desired, by suitable modification of the coefficients of the terms proportional to  $\Delta t^2$ . The rate at which energy is deposited in the electrons in the cell is  $P(0) - P(\Delta t)$ , which can be used as a source term in an electron energy equation.

## 5 Test Cases

Static test cases have been designed and run to check the accuracy of the ray-tracing and power-deposition schemes. To test the ray-tracing algorithm, an  $(l_x \times l_y \times l_z) = (.3 \times .3 \times .3)$  cm box was represented on a uniform 20x2x20 Cartesian grid. The grid was then deformed by imposing random 3D perturbations on all nodes (except those in the  $x = 0, l_x$  and  $z = 0, l_z$  planes) of r.m.s. magnitude  $\simeq .25 \times .3/20$  cm. All internal faces of the resulting mesh were non-planar. An electron density distribution with uniform gradient  $\nabla n_e = (5/2)n_c(\hat{e}_x + \hat{e}_z)$  was laid down on the perturbed mesh, which consequently included part of the critical surface  $x + z = .4$ . Rays were launched from the edge of the mesh at  $z = 0$  in the  $z$ -direction and followed until they reached a boundary face. Comparison of the numerical trajectories with analytic predictions showed agreement to within machine roundoff. The trajectory of a typical ray is shown in Fig. 1.

The power-deposition scheme was tested by tracking the power of a ray that was obliquely incident on a linear density ramp as it traversed the grid. The result is given in Fig. 2, which shows the instantaneous ray power as a function of time, and the power deposited in each cell. Agreement of the numerical and analytic results was again excellent.

## 6 Summary

We have discussed a new package for modeling laser propagation and power deposition on unstructured 3D meshes. Current functionality includes a ray-tracer on arbitrary unstructured 3D meshes composed of hexahedral, prismatic, pyramidal and tetrahedral cells; power deposition by inverse-bremsstrahlung that accounts for strong intra-cellular spatial non-uniformity of the absorption rate; multiple beams whose location, direction, focus, shaped intensity and frequency are user-configurable; computation of the laser-field energy density; and parallelization using MPI and domain decomposition. The package is written in C++ and fully functional in ICF3D with static accuracy tests of the ray-tracer and power deposition, and a number of 2D

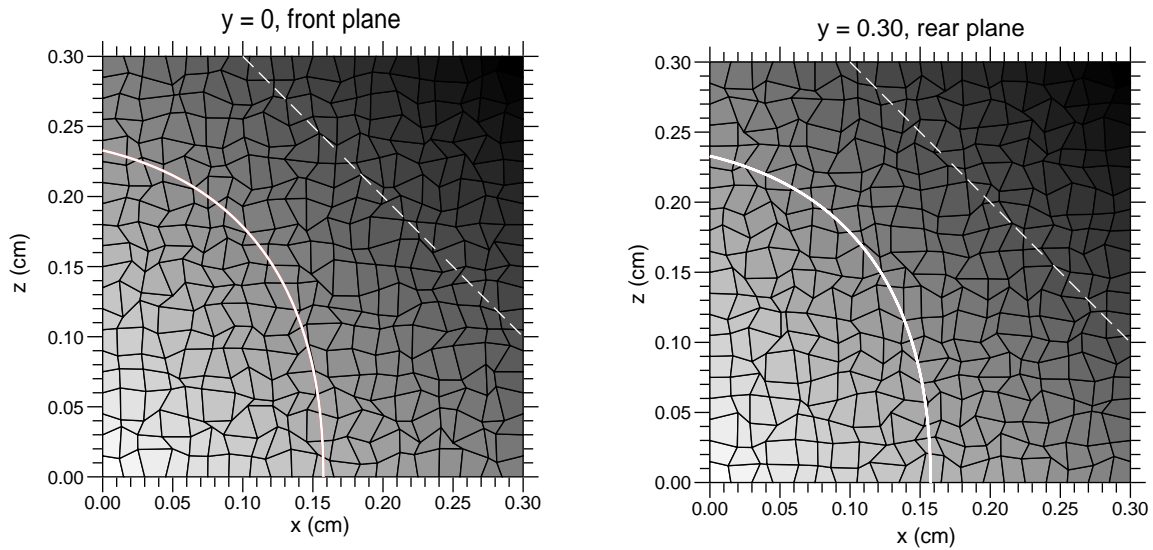


Figure 1: Trajectory of a ray through a randomized 3D mesh (solid white line) projected onto the front and rear grid planes. The average electron density in a zone, which varies from 0.0 on the y-axis to 1.5 critical on the line  $y=0.3$ , is indicated by the gray scale. The critical surface is shown as a white dashed line.

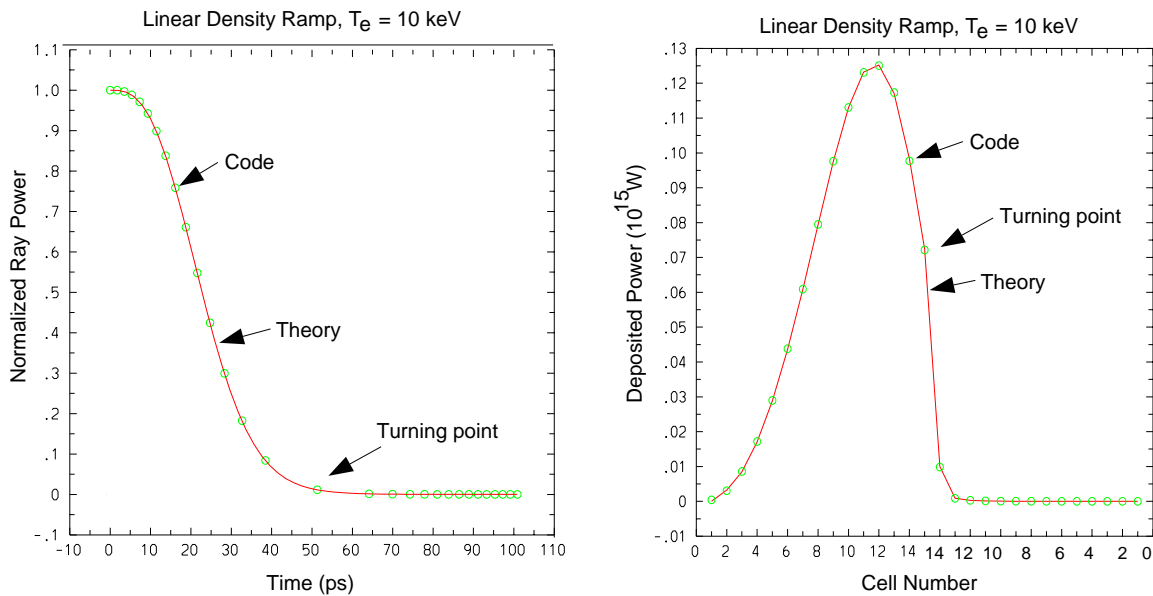


Figure 2: Power deposited by a ray while reflecting from a density ramp. The instantaneous power left in the ray is shown as a function of time on the left, and the power deposited in each cell visited is shown on the right. Open circles indicate the numerical results, while the solid curves result from analytic integration of the deposition rate along the exact ray trajectory.

and 3D laser-driven simulations, one of which is described in a companion paper at this conference[5]. Porting to KULL is in progress, with the package templated on the mesh, initially specialized to “zoo” meshes, and polymeshes to follow.

A more general implementation is currently under construction by G. Kerbel that will be encapsulated in a C++ common library for ease of maintainability, with an API to host codes (*e.g.* KULL, ARES, HYDRA) for flexibility. The library will include built-in parallelization for general architectures using MPI and threads.

## Acknowledgments

We’d like to thank Alex Friedman for access to unpublished work, and Jack Byers, Bruce Cohen, Gary Kerbel, Steve Langer, and George Zimmerman for many helpful discussions. This work was performed under the auspices of the U. S. D. O. E. by the Lawrence Livermore National Laboratory under Contract No. W-7405-ENG-48.

## References

- [1] A. Friedman, *Bull. Am. Phys. Soc.* **28**, 1124 (1983).
- [2] L. D. Landau and E. M. Lifshitz, *Electrodynamics of Continuous Media* (Addison-Wesley, Reading, MA, 1966).
- [3] T. B. Kaiser, “Laser Ray Tracing and Power Deposition on an Unstructured Three-Dimensional Grid,” an expanded version of the present conference report currently in preparation.
- [4] W. L. Kruer, *The Physics of Laser Plasma Interactions* (Addison-Wesley, Redwood City CA, 1988).
- [5] “Simulations of Implosions with a 3D, Parallel, Unstructured-Grid, Radiation-Hydrodynamics Code,” by A. I. Shestakov, J. L. Milovich, M. K. Prasad.